Molecular Neurobiology (2025) 62:7330–7344
https://doi.org/10.1007/s12035-025-04704-z

RESEARCH

The Nerve-Induced Adipose Stem Cells Promote Nerve Repair in Stress Urinary Incontinence by Regulating Schwann Cell Repair Phenotype Conversion Through Activation of the Notch Pathway

Ming Liu[1,2] · Youyi Lu[1] · Fengze Sun[1] · Yongwei Li[1] · Jitao Wu[1] · Qingsong Zou[1]

Received: 10 June 2024 / Accepted: 13 January 2025 / Published online: 30 January 2025

Abstract

Stress urinary incontinence (SUI) currently lacks effective treatment options, and the restoration of neurological function remains a major challenge, with unmet clinical needs. Research has indicated that adipose-derived stem cells (ADSCs) can be induced to differentiate into neural-induced adipose-derived stem cells (NI-ADSCs) under specific inductive conditions, exhibiting excellent neuroregenerative capabilities. ADSCs were obtained from female SD rats and induced into NI-ADSCs. In vitro, NI-ADSCs were co-cultured with Schwann cells (SCs) to investigate their effects on SC proliferation and repair phenotype transition and further explore its underlying mechanism. In vivo, a rat model of SUI was established using a bilateral pudendal nerve transection method. NI-ADSCs were injected into the urethral sphincter to evaluate their effects on urodynamics, muscle angiogenesis, and neural repair in SUI rats, while also exploring the mechanisms of neural repair. This study used EGF, FGF, and B27 to induce ADSCs into NI-ADSCs expressing neural induction markers (MAP, Nestin, and PAX6). In vitro experiments found no significant difference in the proliferation of L6 and RSC96 between NI-ADSCs and ADSCs ($p > 0.05$). However, when co-cultured with NI-ADSCs, SCs showed upregulated expression of repair-related phenotypic markers (BDNF, GDNF, and GFAP). In this phenotypic transformation process, the expression of Notch-related pathway proteins (Notch1, NICD, and Hes1) was increased, and the use of DAPT (a Notch pathway inhibitor) could suppress the SC repair phenotype transformation. In vivo, experiments revealed that intraurethral injection of NI-ADSCs significantly promoted the expression of neural marker (S100β) and demyelination markers (GFAP) and urodynamic recovery in SUI rats, while DAPT inhibited its neural repair effect. In summary, our study demonstrates that NI-ADSCs can promote nerve regeneration by promoting and maintaining the repair-related phenotype of SCs. The underlying mechanism may be related to the activation of the Notch signaling pathway.

Keywords Adipose-derived stem cells · Stress urinary incontinence · Nerve induction · Nerve repair

Introduction

Stress urinary incontinence (SUI) is a common urinary system disorder in women. The main symptom is involuntary urine leakage, which seriously affects the patient's quality of life and health [1]. Currently, the clinical treatments for SUI (including pelvic floor muscle exercises, functional electrical stimulation, biofeedback training, drug therapy, and sling surgery) have not restored the function of the urethral sphincter and its surrounding nerves [2]. Therefore, the clinical efficacy is often poor, and there are many complications. There is an urgent clinical need for a treatment that can fundamentally restore the function of the urethral sphincter and its surrounding nerves.

Ming Liu, Youyi Lu, and Fengze Sun contributed equally to this work as co-first authors.

✉ Jitao Wu
wjturology@163.com

✉ Qingsong Zou
zou_qingsong@126.com

[1] Department of Urology, Yantai Yuhuangding Hospital, Qingdao University, No. 20 East Yuhuangding Road, Yantai 264000, Shandong, China

[2] Second Clinical Medical College, Binzhou Medical University, Yantai 264003, Shandong, China

Stem cell therapy is a promising approach for replacing, repairing, or enhancing the biological function of damaged tissues or organs. Adipose-derived stem cells (ADSCs) have been a research hotspot in the past decade. Adipose stem cells have advantages such as easy accessibility, strong proliferation, and differentiation capabilities. Previous studies have confirmed that they have a significant effect on improving SUI function, but the results of related nerve repair have been unsatisfactory [3, 4].

Neural stem cells have been reported in related research to repair peripheral nerve injuries. However, the difficulty in obtaining neural stem cells and the risk of tumor formation after transplantation have limited their clinical application [5–7]. Although ADSCs are of mesodermal origin and neural cells are of ectodermal origin, numerous studies have reported that ADSCs can be induced to differentiate into neuron-like cells through in vitro trans-germ layer induction [8–10]. The neuron-like cells induced from ADSCs in vitro can express a large number of proteins related to nerve regeneration [11–13]. The induction of ADSCs into neuron-like cells combines the advantages of ADSCs and neural stem cells, providing a new approach for tissue engineering and nerve repair.

Schwann cells (SCs) play a crucial role in the repair of peripheral nerve injuries. When there is peripheral nerve damage, SCs undergo a transformation from a myelinating state to a repair phenotype. They upregulate the expression of immature SC markers such as glial fibrillary acidic protein (GFAP). They also activate various transcription factors (c-JUN, SOX2, and Notch) SCs secrete a range of neurotrophic factors (FGF, NGF, BDNF, and GDNF) to promote axon regeneration [14–16].

The Notch signaling pathway is an evolutionarily conserved key signaling pathway that determines cell fate and influences biological processes such as proliferation, differentiation, and apoptosis in pluripotent stem cells. It consists of Notch receptors, Notch ligands, DNA-binding proteins, effector molecules, and regulatory molecules of Notch [17]. The specific binding of Notch ligands from adjacent cells to receptors leads to the release of the Notch intracellular domain (NICD), which translocates to the nucleus to form a transcription activation complex that regulates Notch-dependent gene expression. Research has shown that the activation of the Notch signaling pathway plays an important role in neurogenesis.

This study aims to investigate the effects of NI-ADSCs injected transurethrally on nerve repair in a rat model of bilateral pudendal nerve transection-induced SUI, as well as its potential mechanisms of action. This research provides a new theoretical basis for stem cell therapy for SUI.

Materials and Methods

Isolation and Cultivation of ADSCs

Two-week-old female SD (Sprague–Dawley) rats were euthanized using cervical dislocation. The abdominal hair of the rats was shaved, and the skin was aseptically disinfected. A 2 cm incision was made on both sides of the groin, and a subcutaneous fat tissue block of approximately 0.5 cm × 0.5 cm × 1 cm was extracted, ensuring the removal of fascial tissue and blood vessels from the surface of the fat. The fat tissue was washed three times with a 0.25% chloramphenicol solution for 1 min each time, followed by rinsing with PBS (phosphate-buffered saline) for 1 min, three times. The washed fat tissue was minced into fragments of approximately 0.1 cm × 0.1 cm × 0.1 cm, and the minced fat tissue fragments were transferred to a 50-ml centrifuge tube. 0.1% type I collagenase, at a volume approximately twice the volume of the fat tissue, was added to the tube. The digestion was carried out under 37 °C conditions with shaking at 150 rpm/min for 1 h. After digestion, an equal volume of cell culture medium was added, and the mixture was filtered through a 100-mesh cell strainer. The filtrate was centrifuged for 5 min at 1500 rpm/min to remove the supernatant, leaving the precipitate. The precipitate was resuspended in 10 ml of low-glucose DMEM (Dulbecco's Modified Eagle Medium) culture medium containing 10% FBS (fetal bovine serum). The cell suspension was seeded in a 100 mm culture dish and incubated in a cell culture incubator (37 °C, 5% CO_2 concentration, 95% humidity) without agitation. The medium was changed after 2 days of incubation.

Identification of Adipogenic and Osteogenic Differentiation Potential of ADSCs

Take the third passage of ADSCs and wait for the cells to reach over 90% confluence. Digest the cells, centrifuge, resuspend, and seed them in a 6-well plate with coverslips at a seeding density of approximately 4×10^3 cells/cm^2. When the ADSCs reach 80% confluence on the coverslips, remove the culture medium from the wells, gently wash with PBS three times for 1 min each, and add about 2 ml of osteogenic induction medium or adipogenic induction medium to each well. Incubate the cells in a 37 °C, 5% CO_2 humidified incubator. Change the medium every 2 days and induce for approximately 3 weeks. After 3 weeks, remove the osteogenic or adipogenic induction medium, and wash the cells on the cover slips with PBS three times for 5 min each. Fix the cells with 4% paraformaldehyde for about 15 min. Wash away the paraformaldehyde with PBS

three times for 5 min each. Proceed with Oil Red O staining and Alizarin Red staining. For Oil Red O staining, add Oil Red O dye (T210421D501, Cyagen) and incubate for 15 min. Rinse with 60% isopropanol for 1 min to remove excess dye. For Alizarin Red staining, add Alizarin Red solution (T210422D501, Cyagen) and incubate for 30 min. Wash with double-distilled water three times, for about 10 s each. Wash with Alizarin Red differentiation solution for one time, approximately 15 s. Finally, wash with PBS three times for 5 min each. Observe and capture images under a microscope.

Flow Cytometry

Take the third passage of ADSCs and wait for the cells to reach over 90% confluence. Digest the cells, centrifuge, resuspend, adjust the cell suspension to a concentration of approximately 1×10^7 cells/ml, and prepare the cell suspension for the examination of stem cell-related antigens CD29 (12–0299-42, Thermo Fisher Scientific), CD44 (12–0441-81, Thermo Fisher Scientific), CD45 (MA5-28679, Thermo Fisher Scientific), and CD90 (11–0900-81, Thermo Fisher Scientific). Take five flow cytometry tubes, add 100 µl of cell suspension to each tube, and add 2 µl of PE-conjugated anti-CD29 antibody, 2 µl of PE-conjugated anti-CD44 antibody, 2 µl of FITC-conjugated anti-CD45 antibody, and 2 µl of FITC-conjugated anti-CD90 antibody to each tube. Mix well, incubate in the dark at room temperature for approximately 30 min, wash with PBS three times for 5 min each, remove the supernatant after centrifugation, resuspend the pellet in 500 µl of PBS, and analyze using a flow cytometer. Analyze 1×10^5 cells in each flow cytometry tube, record the percentage of cells positive for fluorescent antibody staining, and analyze the data using CellQuest software.

Neural Induction of ADSCs

Select the third passage of ADSCs, and seed them in the neural induction medium. Prepare the neural induction medium by supplementing DMEM/F12 (1:1) medium with 20 ng/l of epidermal growth factor (EGF), 20 ng/l of basic fibroblast growth factor (bFGF), and 1% B27 [18–20]. Change the medium every 2 days and observe the cellular morphology under a light microscope.

Cell Co-culture System

We divided the system into a control group, an ADSC group, and an NI-ADSC group. RSC96 or L6 cells were placed in DMEM F12 containing 10% FBS and seeded in the upper chamber of the cell co-culture system. According to the experimental group classification, ADSCs or NI-ADSCs were placed in DMEM F12 without FBS and seeded in the lower chamber, while the control group's lower chamber contained only a serum-free culture medium. The cells were cultured in a 37 °C, 5% CO_2 incubator, with medium changes every 72 h.

For investigating the mechanism of action, we also utilized a cell co-culture system, setting up a control group, NI-ADSC group, and DAPT group. RSC96 cells were placed in DMEM F12 containing 10% FBS and seeded in the upper chamber of a cell co-culture system. NI-ADSCs were seeded in the lower chamber of each experimental group, with the addition of DAPT in the DAPT inhibitor group, while the control group only had RSC96 cells seeded in the upper chamber. The cultural conditions were the same as before.

Cell Proliferation Assay

The Cell Counting Kit-8 (CCK-8) assay was used to measure cell proliferation. RSC96 or L6 cells were plated at a density of 2×10^3 cells per well in 96-well plates. Each well was subsequently incubated at 37 °C for 4 h following an initial incubation for 1, 2, 3, and 4 days. Microplate readers were used to determine the absorbance of each well at 450 nm.

Western Blotting

Western blotting was performed using the standard methods. Total protein was extracted using the Radio Immunoprecipitation Assay (RIPA) Lysis Buffer (Servicebio Technology, China). An equal amount of protein was separated on 7.5%, 10%, and 15% Bis–Tris gels (Thermo Fisher Scientific) and transferred onto a nitrocellulose membrane by electroblotting. The membrane was incubated overnight at 4 °C with the primary antibody, rinsed three times with tris-buffered saline with Tween 20 (TBST), and incubated with a second antibody for 1 h at room temperature the next day. The membranes were then subjected to a developer for imaging using a luminous solution (Affinity Biosciences, Cincinnati, OH, USA). The primary antibodies are presented in Supplementary Table S1. The western blot experiments in each group were repeated at least three times.

Quantitative Real-Time Polymerase Chain Reaction

According to the manufacturer's instructions, RNA was isolated using a TRIzol reagent (Tiangen Biotech, China). The RNA was then reverse transcribed by PrimeScript RT enzyme mix and RT Primer Mix (Accurate Biology, China). Quantitative real-time polymerase chain reaction (qRT-PCR) was applied to quantitative analysis using TB Green Premix Ex Taq II, PCR Primer, and ROX Reference Dye (QIAGEN, Hilden, Germany) on an Automated Thermal Cycler instrument (Thermo Fisher Scientific, Waltham, MA, USA). Rat GAPDH served as the internal control. All qRT-PCR data

were analyzed using the ΔΔCt method. The qRT-PCR primers are presented in Supplementary Table S2. The qRT-PCR experiments were repeated using six biological replicates.

Immunofluorescence Staining of Cell

Immunofluorescence staining was performed to analyze the expression of BDNF (brain-derived neurotrophic factor), GDNF (glial-cell-line-derived neurotrophic factor), and GFAP (glial fibrillary acidic protein) (the antibodies are presented in Supplementary Table S1). Seed the cells in a 24-well plate and culture them in a 37 °C, 5% CO_2 incubator for 2 days. The cells were fixed in 4% paraformaldehyde at room temperature and washed three times with PBS. After 15 min, the cells were permeabilized with 0.5% Triton X-100 (Solarbio Life Sciences, China) for 20 min and washed three times with PBS. After blocking with 5% bovine serum albumin (BSA; Biotopped Life Sciences, China) for 2 h, add the corresponding primary antibody to each well. The cells were then incubated overnight at 4 °C in a wet box. Subsequently, after being rinsed with PBS, the cells were incubated with goat anti-rabbit secondary antibody for 1 h. After washing three times with PBS, stain the cell nuclei with DAPI (4′,6-diamidino-2-phenylindole) staining solution for 15 min. After washing three times with PBS, fluorescent labeling was observed under a fluorescent microscope (ECHO, USA). The immunofluorescence staining experiments in each group were repeated at least three times. The same protocol was applied to neural differentiation.

The Construction and Grouping of SUI Rat Models

The animal experiments were approved by the Yuhuangding Hospital Animal Care and Use Committee in Yantai.

Female SD rats were anesthetized by intraperitoneal injection of 1% pentobarbital (0.3 ml/100 g). A midline incision was made on the back, and muscles were dissected to locate the lumbosacral trunk. The lumbosacral trunk was dissected upwards, revealing the pudendal artery and vein along with the pudendal nerve. The pudendal nerve was then cut with scissors on both sides [21–24]. The incision was sutured, and the rats were returned to the animal facility for further care. SUI rats and sham-operated rats were maintained for an additional 2 weeks before undergoing urodynamic and histological assessments.

Forty 4-week-old female SD rats were randomly divided into four groups: sham surgery group, SUI + PBS injection group, SUI + ADSCs injection group, and SUI + NI-ADSCs injection group. Except for the sham surgery group, all other groups underwent bilateral pudendal nerve transection (PNT). After anesthesia, the rats were laparotomized, the bladder was exposed, and the urethra was separated to reveal the junction of the bladder neck and urethra. The sham operation group did not receive any injection, while the remaining groups were injected with 25 μl of PBS solution, 25 μl of ADSCs solution, or 25 μl of NI-ADSCs solution, respectively, at four points (3, 6, 9, and 12 o'clock positions) on the urethra (0.5 cm away from the junction of the bladder neck and urethra). After 8 weeks of continuous feeding under the same conditions, urodynamic testing was performed on each group, and urethral tissue samples were collected for histological examination.

Histological and Morphological Analysis

The SD rat tissue samples were fixed overnight in 4% paraformaldehyde (PFA), followed by dehydration in a gradient of ethanol and embedding in paraffin. Longitudinal and transverse Sects. (5 μm) were dewaxed and hydrated after paraffin embedding. The tissue sections were stained with hematoxylin–eosin (H&E) and Masson staining as per the manufacturer's instructions. Finally, the slides were fixed with neutral resin and coverslipped. Images of the stained sections were captured using a light microscope.

Tissue Immunofluorescence Staining

The urethral sections were fixed at room temperature with 4% paraformaldehyde (PFA) for 10 min. After permeabilization with 1% Triton X-100 for 15 min, non-specific binding was blocked with 3% BSA for 2 h at 37 °C. Then, samples were incubated with primary antibodies (anti-α-SMA, anti-CD31, anti-S100β, and anti-GFAP antibody) at the appropriate dilution at 4 °C overnight. FITC secondary antibody was used for 1 h at 37 °C after washing with PBS. The specimens were then counterstained for 5 min with the nuclear dye 4′,6-diamidino-2′-phenylindole (DAPI), washed with PBS, and covered with a coverslip, before being examined and imaged using an automatic fluorescence microscope (Axio Observer 7, USA). For determining the mean intensity of α-SMA, CD31, anti-S100β, and GFAP immunofluorescence, five random sections per animal were observed and analyzed using ImageJ software (NIH, USA).

Statistical Analysis

All statistical analyses were conducted using GraphPad Prism 8.0 software (GraphPad Software, San Diego, CA, UA), and a p-value < 0.05 was considered statistically significant ($^{*}p < 0.05$; $^{**}p < 0.01$; $^{***}p < 0.001$).

Result

The Morphology, Differentiation Capacity, and Phenotypic Identification of Adipose-Derived Stem Cells

We obtained inguinal fat tissue from female SD rats and successfully cultured ADSCs using an enzymatic digestion method (Fig. 1A). Initially, the cells exhibited irregular shapes, appearing as short spindle-shaped or polygonal cells (Fig. 1B, C). After the first passage, they were able to reach confluence again within 3 days. We selected P3-ADSCs and induced them with specific adipogenic and osteogenic differentiation media for adipogenic and osteogenic differentiation. Oil Red O staining revealed the presence of red-stained lipid droplets in the cytoplasm of ADSCs, indicating adipogenic differentiation (Fig. 1D). Alizarin Red staining showed orange-red stained calcium deposits outside the cells, indicating osteogenic differentiation (Fig. 1E). This demonstrates that the primary cultured ADSCs possess the multipotent differentiation ability of stem cells. We also selected the 3rd passage of ADSCs and used flow cytometry to detect the expression of stem cell surface markers (CD29, CD44, and CD90) and blood cell surface marker (CD45). The results showed that the positivity rates for CD29, CD44, CD45, and CD90 were 99.96%, 99.41%, 0.15%, and 96.37%, respectively (Fig. 1F). Therefore, the primary cultured ADSCs expressed stem cell markers and did not express blood cell markers, which is consistent with the phenotype of ADSCs.

Inducing ADSCs to Differentiate into NI-ADSCs

We employed a classical and efficient method to induce ADSCs into NI-ADSCs with neuroregenerative capabilities (Fig. 2A). The P3-ADSCs were selected (Fig. 2B), and the culture medium was switched to a serum-free induction medium (DMEM/F12, EGF, bFGF 20 mg/ml supplemented

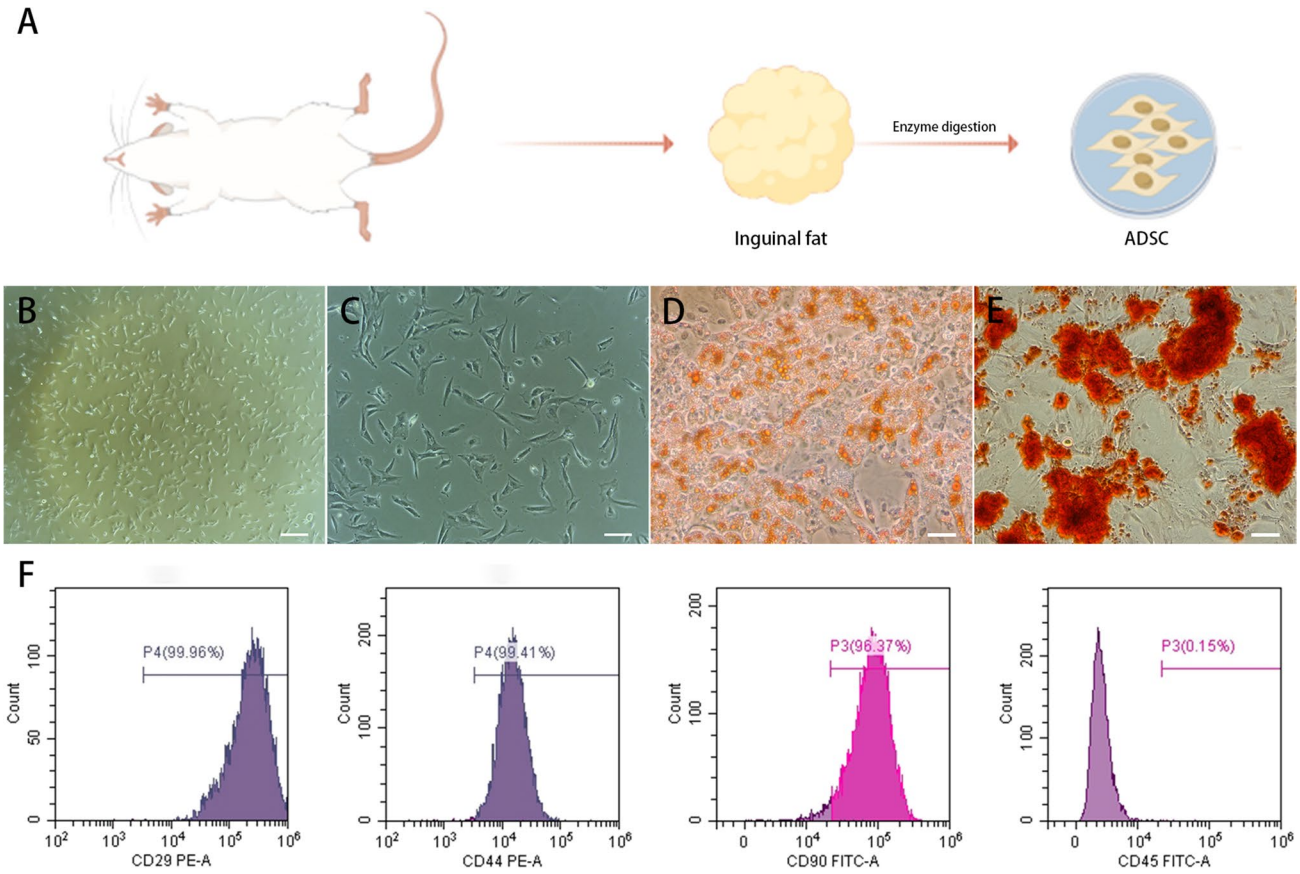

Fig. 1 Identification of ADSCs. **A** Abridged general view of obtaining ADSC from the inguinal fat of a female SD rat. **B**, **C** Observe the morphology of ADSCs under a light microscope, scale bar = 1000 μm or 400 μm. **D** Appearance of red-stained lipid droplets in the cytoplasm using Oil Red O staining. Scale bar = 50 μm. **E** Deposition of orange-red calcium salts outside the cells observed through Alizarin Red staining. Scale bar = 50 μm. **F** The flow cytometry analysis to analyze the cell surface markers CD29, CD44, CD45, and CD90 on ADSCs. Figure 1**A** was generated using Figdraw (www.figdraw.com)

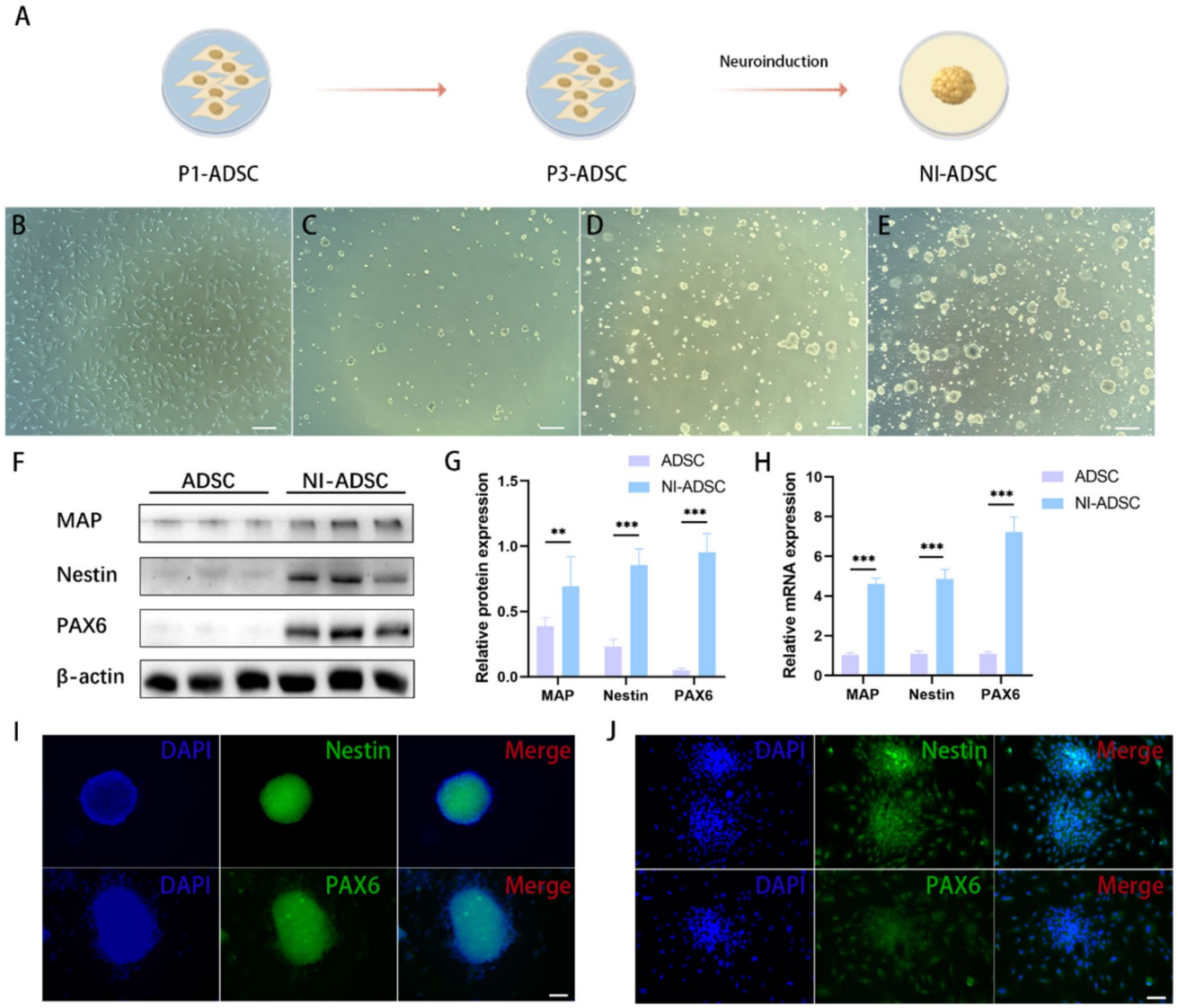

Fig. 2 Induction and characterization of ADSCs for neural differentiation. **A** Abridged general view of neural induction of ADSC into NI-ADSC. **B** Observe the morphology of ADSCs under a light microscope, scale bar = 1000 μm. **C–E** Observe the morphological changes of NI-ADSCs on 2, 4, and 6 days under a light microscope, scale bar = 1000 μm. **F** The protein levels of factors associated with neural induction (MAP, Nestin, and PAX6) were detected by western blot in each group. **G** Quantification of MAP, Nestin, and PAX6 protein levels in each group. The data are expressed as mean ± SD ($n = 3$). **H** The relative mRNA expression of MAP, Nestin, and PAX6 was detected through qRT-PCR. **I** Immunofluorescence staining reveals the expression of Nestin and PAX6 in suspended NI-ADSCs. **J** Immunofluorescence staining reveals the expression of Nestin and PAX6 in adherent NI-ADSCs, bar = 100 μm. Figure 2**A** was generated using Figdraw (www.figdraw.com)

with N2, B27). Under the microscope, ADSCs adhered to the culture dish in a spindle shape, and they gradually aggregated into spherical structures (Fig. 2C–E). We performed PCR and western blot analysis to detect the expression levels of neuroinduction-related markers in ADSCs and NI-ADSCs. The results showed that NI-ADSCs exhibited high expression of MAP, Nestin, and PAX6. We then further conducted immunofluorescence staining on NI-ADSCs. Immunofluorescence staining was conducted on NI-ADSCs, revealing that NI-ADSCs exhibited high expression of the neural stem cell markers MAP, Nestin, and PAX6. In conclusion, we successfully induced ADSCs into NI-ADSCs through cross-lineage induction.

In Vitro Experiments to Validate the Effects of ADSCs and NI-ADSCs on Muscle Regeneration and Neural Repair

To elucidate the effects of ADSCs and NI-ADSCs on muscle regeneration and neural repair, we seeded skeletal

muscle cell line L6 or Schwann cell line RSC96 in the upper chamber of a transwell system and cultured them with a regular culture medium. In the lower chamber, we added PBS, ADSCs, and NI-ADSCs, dividing them into the control group, ADSC group, and NI-ADSC group (Fig. 3A). We conducted in vitro proliferation experiments using CCK-8 assay. The results showed that both ADSCs and NI-ADSCs significantly enhanced the proliferation activity of L6 and RSC96 cells compared to the blank control group (Fig. 3B, C). However, there was no significant difference in the enhancement of proliferation activity between the two groups for L6 and RSC96 cells ($p > 0.05$). We collected RSC96 cells from the control group, ADSC group, and NI-ADSC group for western blotting, qRT-PCR, and immunofluorescence staining. We found that compared to the control group and ADSC group, the NI-ADSC group significantly promoted the expression of phenotype-related markers (GDNF, BDNF, and GFAP) in RSC96 cells (Fig. 3D–G).

NI-ADSCs Promote Schwann Cell Phenotype Transformation Towards a Repair Phenotype by Activating the Notching Pathway

To investigate the mechanism by which NI-ADSCs promote the transformation of RSC96 towards a neural repair phenotype, we divided the cells into control, ADSC, or NI-ADSC group. After co-culturing the cells, we performed western blot analysis on the two groups of RSC96 cells (Fig. 4A, B). We found that NI-ADSCs, compared to the control and ADSC groups, significantly promoted the expression of Notch pathway–related markers (Notch1, NICD, and Hes1) in Schwann cells. To further validate whether the transformation of the repair phenotype is achieved through the activation of the Notch pathway, we added the Notch pathway inhibitor DAPT to the groups previously mentioned (Fig. 4C). After co-culturing the cells, we obtained RSC96 cells from each group for western blot, qRT-PCR,

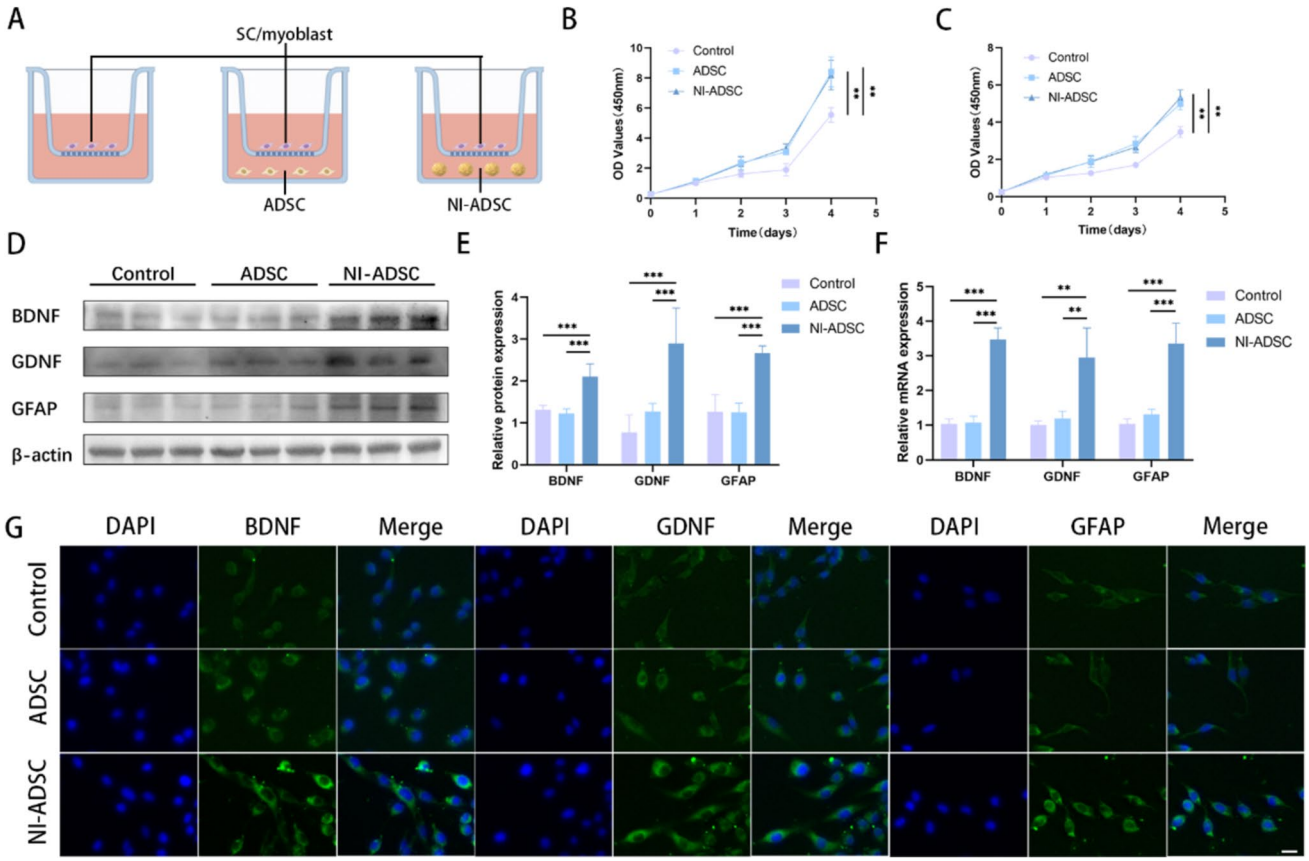

Fig. 3 NI-ADSCs induce repair phenotypic transformation for SCs. **A** Abridged general view of co-culture system SCs, ADSCs, and NI-ADSCs. **B** The effects of ADSC or NI-ADSC on the proliferation ability of RSC96 were analyzed via the CCK-8. **C** The effects of ADSC or NI-ADSC on the proliferation ability of L6 were analyzed via the CCK-8. **D** The protein levels of factors associated with Schwann cell repair phenotype (BDNF, GDNF, and GFAP) were detected by western blot in each group. **E** Quantification of repair of phenotypic-related protein levels in each group. The data are expressed as mean ± SD ($n = 3$). **F** The relative mRNA expression of BDNF, GDNF, and GFAP was detected through qRT-PCR. **G** Immunofluorescence staining was performed to reveal the expression of BDNF, GDNF, and GFAP in the SCs of each group, bar = 50 μm. Figure 3**A** was generated using Figdraw (www.figdraw.com)

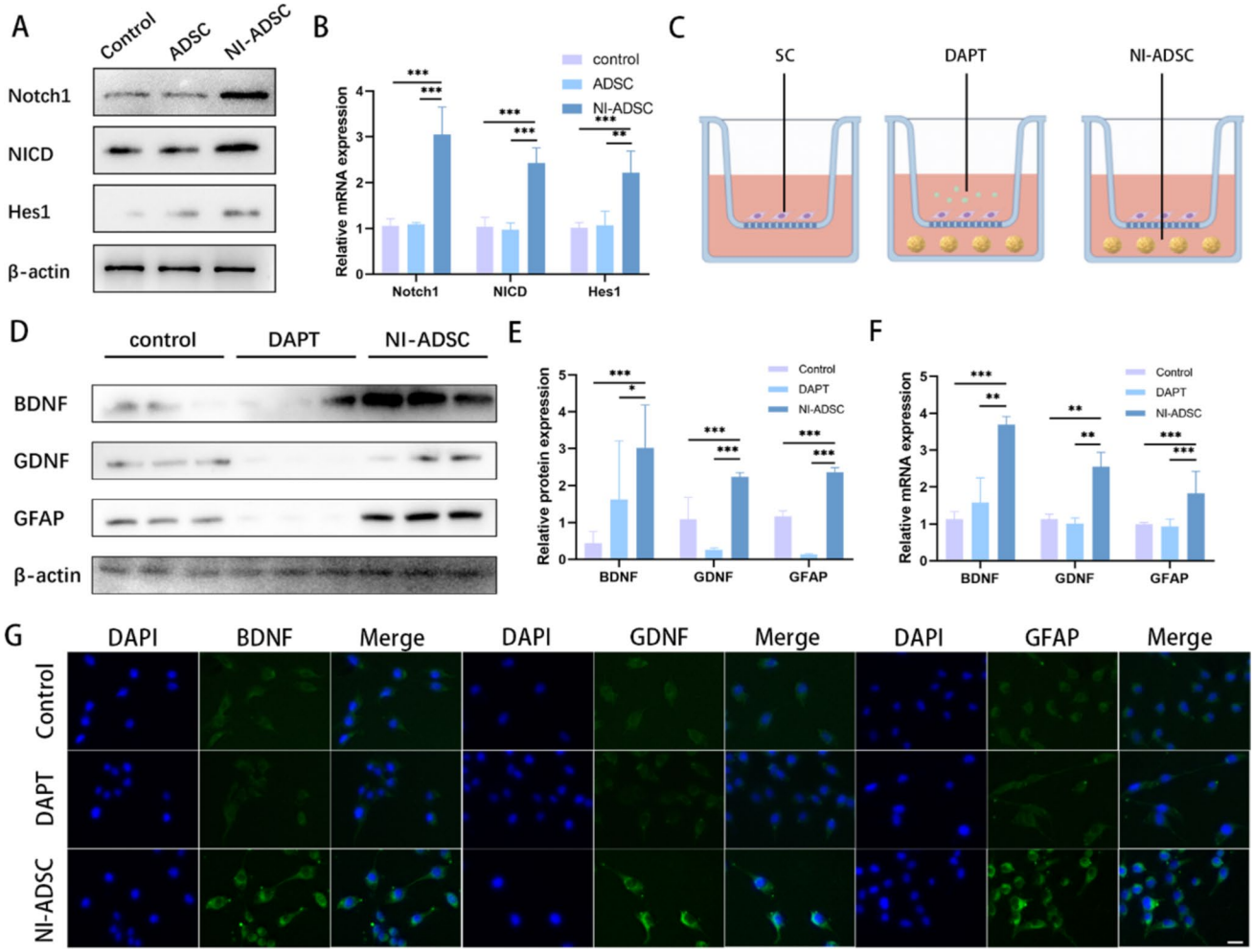

Fig. 4 The Notch signaling pathway is a crucial pathway that promotes the phenotypic transition of SCs related to repair. **A** Western blot analysis to assess the expression levels of Notch pathway–related markers (Notch1, NICD, and Hes1) in SCs from each group. **B** Quantification of Notch pathway–related protein levels in each group. The data are expressed as mean ± SD ($n = 3$). **C** Abridged general view of co-culture system SCs, DAPT, and NI-ADSCs. **D** Western blot analysis to assess the expression levels of Notch pathway–related markers (Notch1, NICD, and Hes1) in SCs from each group. The protein levels of factors associated with the Schwann cell repair phenotype (BDNF, GDNF, and GFAP) were detected by western blot in each group. **E** Quantification of repair of phenotypic-related protein levels in each group. The data are expressed as mean ± SD ($n = 3$). **F** The relative mRNA expression of BDNF, GDNF, and GFAP was detected through qRT-PCR. **G** Immunofluorescence staining was performed to reveal the expression of BDNF, GDNF, and GFAP in the SCs of each group, bar = 50 μm. Figure 4**C** was generated using Figdraw (www.figdraw.com).

and immunofluorescence staining analysis. We found that the addition of DAPT to the culture medium of NI-ADSCs resulted in a decrease in the enhancement of the expression of neural repair-related markers (Fig. 4D–G). Therefore, we speculate that the Notch signaling pathway may play an important role in the transformation of Schwann cells towards a repair phenotype (Fig. 5).

Bilateral Pudendal Nerve Transection Method for Constructing the SUI Rat Model

We established a bilateral pudendal nerve transection SUI animal model in SD rats using the classical method of dorsal incision (Fig. 6A). Two weeks later, histological and urodynamic tests were conducted on the SUI group and the normal group. H&E staining and Masson staining revealed that compared to the normal group, the SUI group exhibited muscle fiber atrophy, disordered arrangement, widened gaps, and enlarged urethral lumen (Fig. 6B). Leak point pressure (LPP) measurements indicated that the average leak point pressure in the SUI group was 22 cmH_2O, while in the normal group, it was 38 cmH_2O, demonstrating a significant difference between the two groups ($p < 0.05$) (Fig. 6G). Immunofluorescence staining showed decreased expression levels of α-SMA (marker of muscle regeneration) CD31 (angiogenesis marker), and

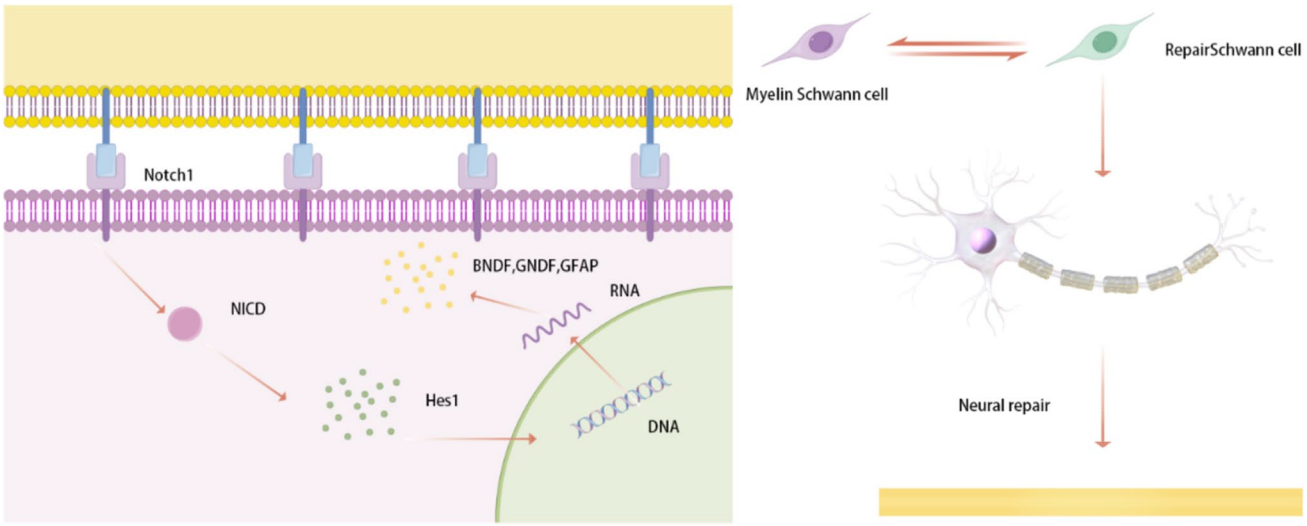

Fig. 5 Schematic diagram of NI-ADSCs activating the Notch pathway to promote nerve regeneration by inducing and maintaining the reparative phenotype of Schwann cells. Figure 5 was generated using Figdraw (www.figdraw.com)

S100β (neural marker) in the SUI group compared to the normal group (Fig. 6C–F). The bilateral pudendal nerve transection urinary incontinence animal model was successfully established.

In Vivo Experiments Investigating the Effects of ADSCs and NI-ADSCs on the SUI Model

We divided the rats into the sham group, SUI group, ADSC group, NI-ADSC, and DAPT group and injected PBS, ADSCs, NI-ADSCs, and NI-ADSCs + DAPT into the urethral sphincter muscle, respectively (Fig. 6A). Eight weeks later, leak point pressure measurements were conducted in each group. We found that the LPP in the ADSC group and the NI-ADSC group was higher than that in the SUI animal model group, approaching levels similar to the sham group, with statistical significance (Fig. 7E). H&E staining and Masson staining showed that after injection of ADSCs and NI-ADSCs, the muscle fibers in SUI rats were arranged neatly, with reduced gaps and a smaller urethral lumen (Fig. 7A). Immunofluorescence staining revealed significantly improved expressions of α-SMA, CD31, GFAP (demyelination marker), and S100β in the ADSC and NI-ADSC groups compared to the SUI group (Figs. 7B–D and 8A–D). Notably, the NI-ADSC group exhibited higher GFAP and S100β expression than the ADSC group (Fig. 8A–D). After the addition of Notch pathway inhibitors, the LPP and the expression of neural and neural repair-related markers in the SUI rats in the NI-ADSCs group were reduced (Fig. 8A–D). NI-ADSCs may promote neural repair in SUI rats by activating the Notch pathway.

Discussion

Stress urinary incontinence (SUI) is a common urinary system disease in women that seriously threatens the physical and mental health of women worldwide. Epidemiological studies have shown that about 200 million women worldwide suffer from urinary incontinence, half of whom has SUI [25, 26]. SUI is the result of the comprehensive effects of factors such as vascular, neurological, and muscular damage. Currently, the main treatment method for SUI is mid-urethral sling surgery [27]. However, the traditional treatment methods for SUI only focus on the reconstruction of the urethral structure, ignoring the repair of nerves, blood vessels, and muscles.

With the rapid development of organizational engineering technology, stem cell therapy has shown certain potential in the treatment of SUI [28]. Research has found that stem cells can significantly improve vascular and muscle damage in SUI, but the treatment effect on SUI nerve damage is limited [29–32]. Studies have found that NSCs can effectively promote the repair of damaged nerves [5, 6, 33]. However, NSCs are difficult to obtain, and there is a risk of tumor formation after transplantation, making it difficult to apply them in the treatment of SUI [7]. ADSCs have advantages such as easy acquisition, minimal trauma, abundant cell numbers, and fewer ethical conflicts, and the method is relatively mature [34]. Research has reported that ADSCs can be induced into NI-ADSCs, which have neural stem cell–related characteristics and can secrete neurotrophic factors to promote nerve regeneration. Currently, there are various methods for inducing stem cells into neurosphere-like cells, most of which have been validated multiple times as reliable induction methods. ADSCs respond well to neuronal

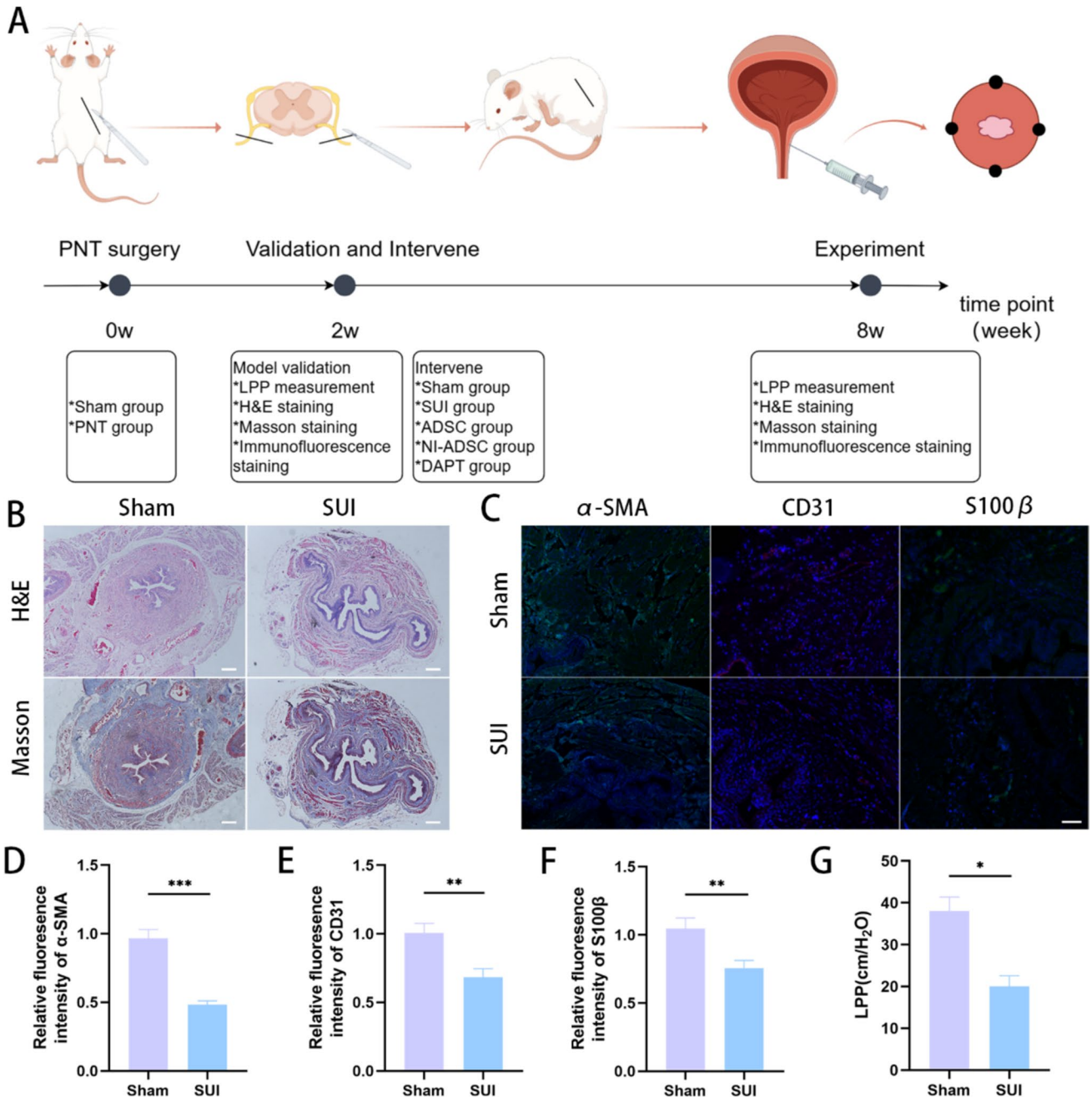

Fig. 6 Establishment and identification of an SUI rat model using PNT. **A** Abridged general view of constructing an SUI rat model through bilateral pudendal nerve transection and a detailed timeline of the rat experiment. **B** Histological examination of urethral tissues in the sham group and the SUI group using H&E and Masson staining, bar = 100 μm. **C** Immunofluorescence staining to detect the expression of SMA-α CD31 and S100β in the urethral tissues of rats in the sham group and the SUI group, bar = 50 μm. **D** Bar graphs showing the mean immunofluorescence intensity of α-SMA in each group ($n = 5$). **E** Bar graphs showing the mean immunofluorescence intensity of CD31 in each group ($n = 5$). **F** Bar graphs showing the mean immunofluorescence intensity of S100β in each group ($n = 5$). **G** The LPP of each group ($n = 5$). Figure 6**A** was generated using Figdraw (www.figdraw.com)

induction methods and can exhibit a high differentiation rate in a relatively short period of time. Ahmadi and others compared two neural induction methods for ADSCs and found that the differentiation of ADSCs into NI-ADSCs was rapid and transient under the chemical induction scheme, while the formation of neurospheres resulted in stable NI-ADSCs [10]. We isolated ADSCs from the inguinal fat tissue of female SD rats and identified their stem cell characteristics through flow cytometry and osteogenic and adipogenic differentiation, confirming that we did obtain ADSCs. Subsequently,

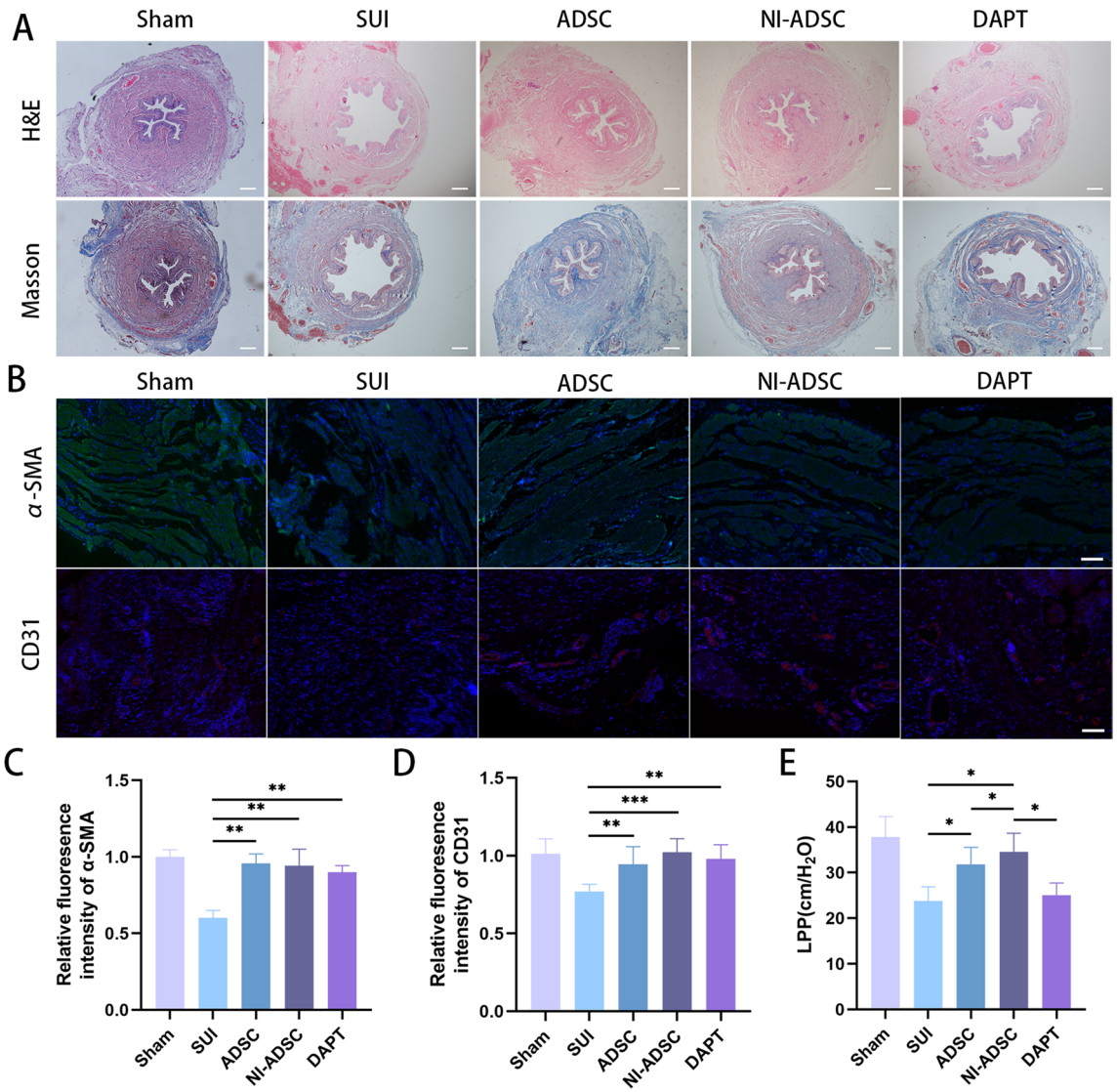

Fig. 7 An in vivo experiment to explore the effects and mechanisms of NI-ADSC on the repair of SUI rats. **A** Histological examination of urethral tissues in each group using H&E and Masson staining, bar = 100 μm. **B** Immunofluorescence staining to detect the expression of α-SMA and CD31 in the urethral tissues of rats in each group, bar = 50 μm. **C** Bar graphs showing the mean immunofluorescence intensity of α-SMA in each group ($n = 5$). **D** Bar graphs showing the mean immunofluorescence intensity of CD31 in each group ($n = 5$). **E** The LPP of each group ($n = 5$)

we successfully induced ADSCs into NI-ADSCs using the classic ADSC neural induction scheme and confirmed their morphological and molecular characteristics through morphology, qRT-PCR, WB, and immunofluorescence.

To further verify the role of NI-ADSCs in nerve repair, we reviewed previous research literature on peripheral nerve injury and found that most in vitro experiments were based on Schwann cells (SCs) [13, 35–37]. SCs are the key glial cells in the peripheral nervous system and play an important role in the repair of peripheral nerve injuries. When the peripheral nerve is injured, Wallerian degeneration and axonal disintegration occur, and the myelinating or Remak Schwann cells undergo a transition to a repair phenotype. The repair phenotype Schwann cells undergo autophagy to clear the myelin and highly express immature Schwann cell markers such as GFAP, p75NTR, and NCAM, which are suppressed during myelination. They also activate various transcription factors (c-JUN, SOX2, Notch, etc.) and cytokines (TNFα, LIF, IL-1α, IL-1β, LIF, and MCP-1) and secrete a series of neurotrophic factors (FGF, NGF, BDNF, GDNF, p75NTR, VEGF, and NT3) to promote myelin degradation, axonal regeneration, and structural reconstruction [13–16]. Therefore, we selected the rat Schwann cell line RSC96 as the target cell. We co-cultured RSC96 with ADSCs and NI-ADSCs, respectively, and used the CCK-8 assay to detect the ability of ADSCs and NI-ADSCs to

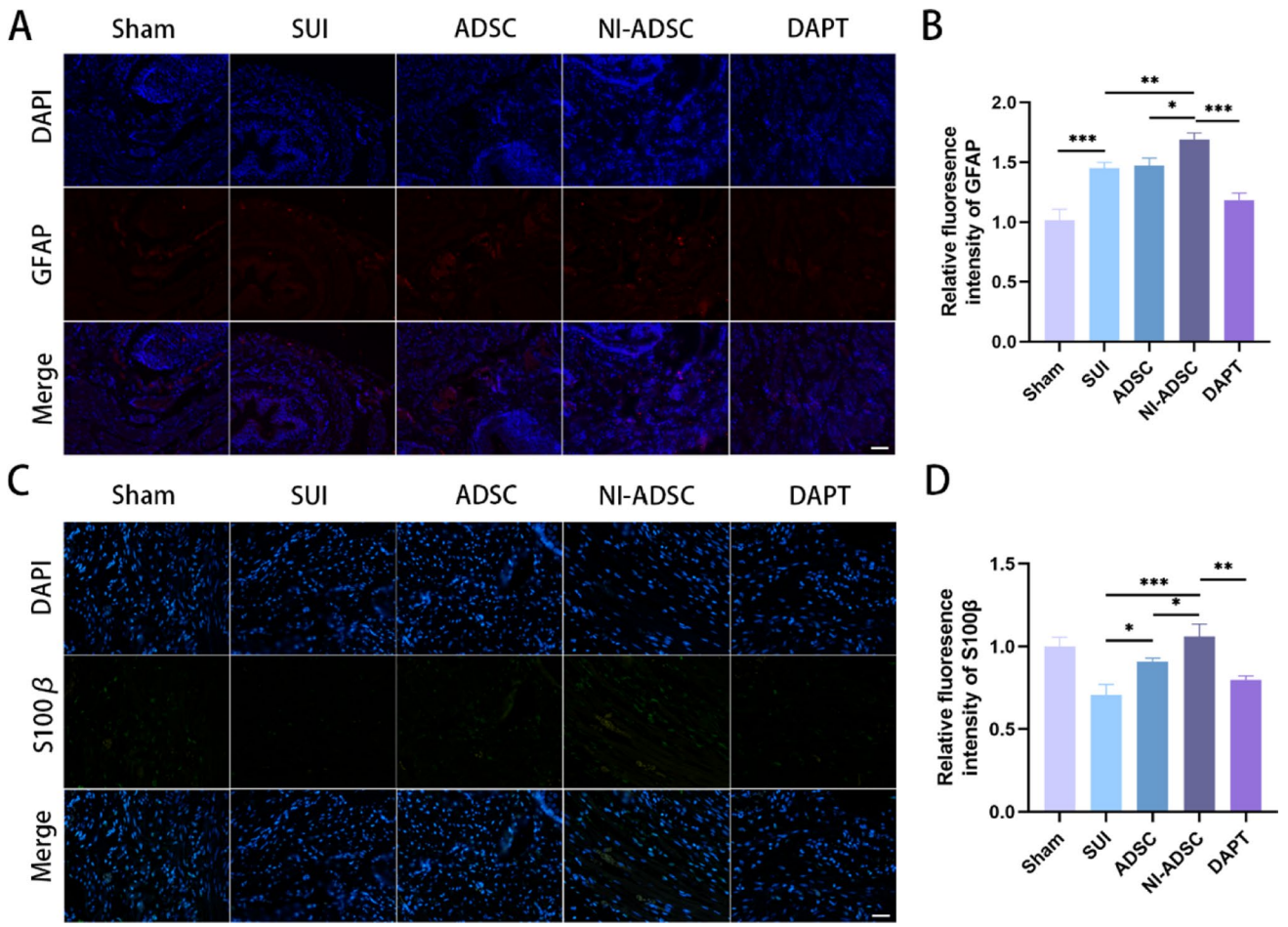

Fig. 8 Nerve repair in rat urethral tissue. **A** Immunofluorescence staining to detect the expression of GFAP in the urethral tissues of rats in each group, scale bar = 50 μm. **B** Bar graphs showing the mean immunofluorescence intensity of GFAP in each group ($n = 5$). **C** Immunofluorescence staining to detect the expression of S100β in the urethral tissues of rats in each group, bar = 50 μm. **D** Bar graphs showing the mean immunofluorescence intensity of S100β in each group ($n = 5$)

promote SC proliferation, and the results showed no significant difference between the two. We used qRT-PCR, WB, and immunofluorescence staining to detect the expression levels of related repair phenotype markers in each group of RSC96. We found that, compared with the control group and the ADSC group, the expression levels of repair phenotype-related genes BDNF, GDNF, and GFAP were significantly increased. This suggests that NI-ADSCs promoted the transition of SCs to the repair phenotype. However, the mechanism by which NI-ADSCs promote the transition of SCs to the repair phenotype is still unclear.

In reviewing the literature on nerve repair and SC phenotype transformation, we found that many pathways affect the transformation of SC phenotypes [13, 38–40]. Notch signaling plays a key role in various biological processes such as the maintenance, proliferation, differentiation, and apoptosis of neural stem cells [17, 41–43]. Notch is a transmembrane protein receptor that is activated through interaction with ligands. Activated Notch is cleaved multiple times by γ-secretase, releasing its intracellular domain (NICD), which then translocates to the cell nucleus and forms a transcription factor that stimulates the transcription of Hes and Hey, thereby regulating downstream target genes. Increasing evidence suggests that the Notch pathway is of great importance in nerve repair. Notch1 is a negative regulator of myelination, promoting or maintaining an immature or dedifferentiated cell state [44, 45]. After nerve injury, Notch expression in the nerve is upregulated, accelerating Schwann cell dedifferentiation, downregulating myelination-related factors, and upregulating axonal regeneration-related factors, thereby promoting nerve repair.

To further understand the potential molecular mechanism by which NI-ADSCs promote the transition of SCs to the repair phenotype, we evaluated the involvement of the Notch signaling pathway. In our study, after co-culturing RSC96 with NI-ADSCs, we used WB to analyze the expression of Notch 1, NICD, and Hes1 at the protein level. The results showed that, compared to the RSC96 cultured alone and

the ADSC group, the expression levels of Notch1, NICD, and Hes1 were significantly increased in the RSC96 group co-cultured with NI-ADSCs. This suggests that the mechanism by which NI-ADSCs promote the transition of SCs to the repair phenotype may involve the activation of the Notch pathway. DAPT is an γ-secretase inhibitor that can inhibit Notch cleavage and is commonly used as a Notch signal inhibitor [46]. We added DAPT to the co-culture of RSC96 and NI-ADSCs. After inhibiting the Notch signal with DAPT, we re-detected the expression levels of SC repair phenotype-related markers and found that at both the mRNA and protein levels, the expression levels in the DAPT group were significantly lower than in the NI-ADSC group. These findings suggest that DAPT can block the Notch signaling pathway, thereby reversing the role of NI-ADSCs in promoting the transition of SCs towards a reparative phenotype. Therefore, it can be seen that the role of NI-ADSCs in promoting the transition of SCs to the repair phenotype is mediated through the activation of the Notch pathway.

The successful establishment of SUI models is fundamental to conducting in vivo studies. At present, there are two main methods to establish SUI rat models: denervation and simulated birth injury. Denervation is dominated by bilateral pudendal nerve severance [21]. It directly cuts the nerve, resulting in neuropathic atrophy of the urethral sphincter [47, 48]. This method is highly specific and has a long maintenance time. Simulated birth injuries are dominated by vaginal dilation (VD), which mimics vaginal delivery, resulting in damage to the urethral neuromuscular and pelvic floor support structures [49]. This method is simple to operate, but there are large individual differences, and the model maintenance time is short. To reduce the adverse effect of the modeling method on the experimental results, we established the SUI rat model using the classical bilateral pudendal neurotomy method. The primary measure for evaluating models of stress urinary incontinence is urodynamics. Currently, leak point pressure (LPP) is considered a reliable method for assessing urethral resistance in SUI models [49]. LPP is bladder pressure with urinary leakage that occurs with increased abdominal pressure, reflects the contractile capacity of the urethral sphincter, has good repeatability, and can be used to evaluate the success of the establishment of animal models of SUI. The results showed that the LPP of SUI rats was significantly lower than that of the sham group after bilateral pudendal nerve cuts, indicating that our SUI rat model was successfully established. To evaluate the efficacy of ADSCs and NI-ADSCs in the treatment of SUI, we divided the rats into five groups: the sham group, the SUI group, the ADSC group, the NI-ADSC group, and the DAPT group, which were injected with PBS, PBS, ADSCs, NI-ADSCs, and NI-ADSCs + DAPT, respectively. After injection for some time, we performed immunofluorescence staining on SUI rats to detect relevant biomarkers of angiogenesis, muscle regeneration, and nerve repair. We found no significant differences in vascularization and muscle regeneration between the ADSC and NI-ADSC groups. Notably, the expression of nerve repair proteins was higher in the NI-ADSC group than in the ADSC group. This suggests that NI-ADSCs may be more repairable than ADSCs in terms of nerve repair. After the addition of Notch pathway inhibitors, the LPP and the expression of neural and neural repair-related markers in the SUI rats in the NI-ADSCs group were reduced. NI-ADSCs may promote neural repair in SUI rats by activating the Notch pathway. This further validates the results of the in vitro experiments.

This study has several limitations. First, stem cell therapy has risks, and direct application of stem cells may have risks such as tumor formation. Current research shows that the main way stem cells exert therapeutic effects is through the secretion of extracellular vesicles that act on target cells. The use of extracellular vesicles derived from NI-ADSCs may maintain the therapeutic effect of cell therapy while reducing the risks associated with cell therapy. Secondly, when conducting in vitro experiments using the transwell system, DAPT may also have potential effects on NI-ADSCs. At present, we are extracting exosomes from NI-ADSCs and conducting an in-depth exploration of the potential nerve repair factors secreted by NI-ADSCs, as well as their mechanism of activating the Notch pathway. Finally, this study is only an animal experiment, and further in vivo experiments are still needed to verify its therapeutic efficacy and safety in clinical settings. We look forward to providing new directions and a more theoretical basis for the clinical treatment of SUI.

Conclusion

In this study, we isolated ADSCs from female SD rats, induced them into NI-ADSCs, and determined the beneficial effects of NI-ADSCs on SC repair-related phenotypes by activating the Notch1 signaling pathway. We hope this study can provide a valuable therapeutic strategy for the neuroregeneration and repair of SUI.

Supplementary Information The online version contains supplementary material available at https://doi.org/10.1007/s12035-025-04704-z.

Acknowledgements We thank the participants of the study.

Author Contributions Ming Liu: Writing – original draft, Methodology, Formal analysis, Data curation. Youyi Lu: Methodology, Investigation. Fengze Sun: Software, Methodology, Investigation. Yongwei Li: Validation, Methodology. Jitao Wu: Supervision, Conceptualization. Qingsong Zou: Writing – review & editing, Supervision, Conceptualization.

Funding This work was supported by the National Natural Science Foundation of China (Nos. 82370690, 82000649, 82270722), the Natural Science Foundation of Shandong Province (No. ZR2023MH241),

and the Taishan Scholars Program of Shandong Province (No. tsqn201909199).

Data Availability No datasets were generated or analysed during the current study.

Declarations

Ethics Approval All related experiments were monitored and approved by the Yuhuangding Hospital Animal Care and Use Committee in Yantai (No. 2024–493).

Consent to Participate All participants were acknowledged and consent to the study, and written informed consent was obtained from all participants.

Consent for Publication All authors consented to the publication of related findings in this study.

Competing Interests The authors declare no competing interests.

References

1. Vaughan CP, Markland AD (2020) Urinary incontinence in women. Ann Intern Med 172(3):Itc17-itc32. https://doi.org/10.7326/aitc202002040
2. Bullock TL, Ghoniem G, Klutke CG, Staskin DR (2006) Advances in female stress urinary incontinence: mid-urethral slings. BJU Int 98 Suppl 1:32–40. https://doi.org/10.1111/j.1464-410X.2006.06361.x. (discussion 1-2)
3. Cui L, Meng Q, Wen J, Gao Z, Yan Z, Tian Y et al (2018) A functional comparison of treatment of intrinsic sphincter deficiency with muscle-derived and adipose tissue-derived stem cells. IUBMB Life 70(10):976–984. https://doi.org/10.1002/iub.1896
4. Li M, Li G, Lei H, Guan R, Yang B, Gao Z et al (2016) Therapeutic potential of adipose-derived stem cell-based microtissues in a rat model of stress urinary incontinence. Urology 97:277.e1-.e7. https://doi.org/10.1016/j.urology.2016.08.009
5. Lee DC, Chen JH, Hsu TY, Chang LH, Chang H, Chi YH et al (2017) Neural stem cells promote nerve regeneration through IL12-induced Schwann cell differentiation. Mol Cell Neurosci 79:1–11. https://doi.org/10.1016/j.mcn.2016.11.007
6. Binan L, Tendey C, De Crescenzo G, El Ayoubi R, Ajji A, Jolicoeur M (2014) Differentiation of neuronal stem cells into motor neurons using electrospun poly-L-lactic acid/gelatin scaffold. Biomaterials 35(2):664–674. https://doi.org/10.1016/j.biomaterials.2013.09.097
7. Jiang L, Jones S, Jia X (2017) Stem cell transplantation for peripheral nerve regeneration: current options and opportunities. Int J Mol Sci 18(1):94. https://doi.org/10.3390/ijms18010094
8. Jang S, Park JS, Jeong HS (2015) Neural differentiation of human adipose tissue-derived stem cells involves activation of the Wnt5a/JNK signalling. Stem Cells Int 2015:178618. https://doi.org/10.1155/2015/178618
9. Razavi S, Razavi MR, ZarkeshEsfahani H, Kazemi M, Mostafavi FS (2013) Comparing brain-derived neurotrophic factor and ciliary neurotrophic factor secretion of induced neurotrophic factor secreting cells from human adipose and bone marrow-derived stem cells. Dev Growth Differ 55(6):648–655. https://doi.org/10.1111/dgd.12072
10. Ahmadi N, Razavi S, Kazemi M, Oryan S (2012) Stability of neural differentiation in human adipose derived stem cells by two induction protocols. Tissue Cell 44(2):87–94. https://doi.org/10.1016/j.tice.2011.11.006
11. Santos J, Milthorpe BK, Herbert BR, Padula MP (2017) Proteomic analysis of human adipose derived stem cells during small molecule chemical stimulated pre-neuronal differentiation. Int J Stem Cells 10(2):193–217. https://doi.org/10.15283/ijsc17036
12. Santos J, Milthorpe BK, Padula MP (2019) Proteomic analysis of cyclic ketamine compounds ability to induce neural differentiation in human adult mesenchymal stem cells. Int J Mol Sci 20(3):523. https://doi.org/10.3390/ijms20030523
13. Huang J, Zhang G, Li S, Li J, Wang W, Xue J et al (2023) Endothelial cell-derived exosomes boost and maintain repair-related phenotypes of Schwann cells via miR199-5p to promote nerve regeneration. J Nanobiotechnol 21(1):10. https://doi.org/10.1186/s12951-023-01767-9
14. Lehmann HC, Höke A (2016) Use of engineered Schwann cells in peripheral neuropathy: hopes and hazards. Brain Res 1638(Pt A):97–104. https://doi.org/10.1016/j.brainres.2015.10.040
15. La Noce M, Mele L, Tirino V, Paino F, De Rosa A, Naddeo P et al (2014) Neural crest stem cell population in craniomaxillofacial development and tissue repair. Eur Cells Mater 28:348–57. https://doi.org/10.22203/ecm.v028a24
16. Taha MF, Javeri A, Kheirkhah O, Majidizadeh T, Khalatbary AR (2014) Neural differentiation of mouse embryonic and mesenchymal stem cells in a simple medium containing synthetic serum replacement. J Biotechnol 172:1–10. https://doi.org/10.1016/j.jbiotec.2013.11.028
17. Yang L, Shen XM, Wang ZF, Li K, Wang W (2022) The Notch signalling pathway and miRNA regulation play important roles in the differentiation of Schwann cells from adipose-derived stem cells. Lab Investig J Tech Methods Pathol 102(3):320–8. https://doi.org/10.1038/s41374-021-00687-2
18. Zhang HT, Liu ZL, Yao XQ, Yang ZJ, Xu RX (2012) Neural differentiation ability of mesenchymal stromal cells from bone marrow and adipose tissue: a comparative study. Cytotherapy 14(10):1203–1214. https://doi.org/10.3109/14653249.2012.711470
19. Xu Y, Liu Z, Liu L, Zhao C, Xiong F, Zhou C et al (2008) Neurospheres from rat adipose-derived stem cells could be induced into functional Schwann cell-like cells in vitro. BMC Neurosci 9:21. https://doi.org/10.1186/1471-2202-9-21
20. Qin Y, Zhou C, Wang N, Yang H, Gao WQ (2015) Conversion of adipose tissue-derived mesenchymal stem cells to neural stem cell-like cells by a single transcription factor, Sox2. Cell Reprogram 17(3):221–226. https://doi.org/10.1089/cell.2015.0001
21. Herrera-Imbroda B, Lara MF, Izeta A, Sievert KD, Hart ML (2015) Stress urinary incontinence animal models as a tool to study cell-based regenerative therapies targeting the urethral

sphincter. Adv Drug Deliv Rev 82–83:106–116. https://doi.org/10.1016/j.addr.2014.10.018
22 Khorramirouz R, Mozafarpour S, Kameli SM, LadiSeyedian SS, Oveisi N, Rahimi Z et al (2016) A novel method of urinary sphincter deficiency: serial histopathology evaluation in a rat model of urinary incontinence. Anat Record (Hoboken, NJ: 2007) 299(2):173–80. https://doi.org/10.1002/ar.23291
23. Wu G, Song Y, Zheng X, Jiang Z (2011) Adipose-derived stromal cell transplantation for treatment of stress urinary incontinence. Tissue Cell 43(4):246–253. https://doi.org/10.1016/j.tice.2011.04.003
24. Jalali Tehrani H, Daryabari SS, Fendereski K, AlijaniZirdehi M, Kajbafzadeh AM (2021) Application of adipose-derived, muscle-derived, and co-cultured stem cells for the treatment of stress urinary incontinence in rat models. Lower Urinary Tract Symptoms 13(2):308–318. https://doi.org/10.1111/luts.12360
25. Xue K, Palmer MH, Zhou F (2020) Prevalence and associated factors of urinary incontinence in women living in China: a literature review. BMC Urol 20(1):159. https://doi.org/10.1186/s12894-020-00735-x
26. Lukacz ES, Santiago-Lastra Y, Albo ME, Brubaker L (2017) Urinary incontinence in women: a review. JAMA 318(16):1592–1604. https://doi.org/10.1001/jama.2017.12137
27 Harland N, Walz S, Eberli D, Schmid FA, Aicher WK, Stenzl A et al (2023) Stress urinary incontinence: an unsolved clinical challenge. Biomed 11(9):2486. https://doi.org/10.3390/biomedicines11092486
28. Liu X, Li T, Zhang J, Lin X, Wang W, Fan X et al (2023) Mesenchymal stem cell-based therapy for female stress urinary incontinence. Front cell Dev Biol 11:1007703. https://doi.org/10.3389/fcell.2023.1007703
29. Wang L, Wang Y, Xiang Y, Ma J, Zhang H, Dai J et al (2021) An in vitro study on extracellular vesicles from adipose-derived mesenchymal stem cells in protecting stress urinary incontinence through microRNA-93/F3 axis. Front Endocrinol 12:693977. https://doi.org/10.3389/fendo.2021.693977
30. Zordani A, Pisciotta A, Bertoni L, Bertani G, Vallarola A, Giuliani D et al (2019) Regenerative potential of human dental pulp stem cells in the treatment of stress urinary incontinence: In vitro and in vivo study. Cell Prolif 52(6):e12675. https://doi.org/10.1111/cpr.12675
31. Fang J, Peng T, Liu J, Liu H, Liu T, Zhang Z et al (2022) Muscle-derived stem cells combined with nerve growth factor transplantation in the treatment of stress urinary incontinence. Urology 166:126–132. https://doi.org/10.1016/j.urology.2022.04.014
32. Li G, Yu C, Yu P, Peng Q, Wang Q, Ren S et al (2022) Periurethral and intravenous injections of adipose-derived stem cells to promote local tissue recovery in a rat model of stress urinary incontinence. Urology 167:82–89. https://doi.org/10.1016/j.urology.2022.05.018
33. Chang J, Li Y, Shan X, Chen X, Yan X, Liu J et al (2024) Neural stem cells promote neuroplasticity: a promising therapeutic strategy for the treatment of Alzheimer's disease. Neural Regen Res 19(3):619–628. https://doi.org/10.4103/1673-5374.380874
34. Dong L, Li X, Leng W, Guo Z, Cai T, Ji X et al (2023) Adipose stem cells in tissue regeneration and repair: from bench to bedside. Regen Ther 24:547–560. https://doi.org/10.1016/j.reth.2023.09.014
35. Seung Lee W, Hong MP, Hoon Kim T, Kyoo Shin Y, Soo Lee C, Park M et al (2005) Effects of lysophosphatidic acid on sodium currents in rat dorsal root ganglion neurons. Brain Res 1035(1):100–104. https://doi.org/10.1016/j.brainres.2004.12.026
36. Wood MD, Willits RK (2009) Applied electric field enhances DRG neurite growth: influence of stimulation media, surface coating and growth supplements. J Neural Eng 6(4):046003. https://doi.org/10.1088/1741-2560/6/4/046003
37. Ben-Zvi A, Yagil Z, Hagalili Y, Klein H, Lerman O, Behar O (2006) Semaphorin 3A and neurotrophins: a balance between apoptosis and survival signaling in embryonic DRG neurons. J Neurochem 96(2):585–597. https://doi.org/10.1111/j.1471-4159.2005.03580.x
38. Xu X, Song L, Li Y, Guo J, Huang S, Du S et al (2023) Neurotrophin-3 promotes peripheral nerve regeneration by maintaining a repair state of Schwann cells after chronic denervation via the TrkC/ERK/c-Jun pathway. J Transl Med 21(1):733. https://doi.org/10.1186/s12967-023-04609-2
39. Pandey S, Mudgal J (2022) A review on the role of endogenous neurotrophins and Schwann cells in axonal regeneration. J Neuroimmune Pharmacol Off J Soc NeuroImmune Pharmacol 17(3–4):398–408. https://doi.org/10.1007/s11481-021-10034-3
40. Liu T, Wang Y, Lu L, Liu Y (2022) SPIONs mediated magnetic actuation promotes nerve regeneration by inducing and maintaining repair-supportive phenotypes in Schwann cells. J Nanobiotechnol 20(1):159. https://doi.org/10.1186/s12951-022-01337-5
41. Piovesana R, Pisano A, Loreti S, Ricordy R, Talora C, Tata AM (2022) Notch signal mediates the cross-interaction between M2 muscarinic acetylcholine receptor and neuregulin/ErbB pathway: effects on Schwann cell proliferation. Biomolecules 12(2):239. https://doi.org/10.3390/biom12020239
42. Wang W, Gu MF, Wang ZF, Shen XM, Zhang J, Yang L (2021) Let-7a-5p regulated by lncRNA-MEG3 promotes functional differentiation to Schwann cells from adipose derived stem cells via directly inhibiting RBPJ-mediating Notch pathway. Apoptosis Int J Programmed Cell Death 26(9–10):548–560. https://doi.org/10.1007/s10495-021-01685-x
43. Lampada A, Taylor V (2023) Notch signaling as a master regulator of adult neurogenesis. Front Neurosci 17:1179011. https://doi.org/10.3389/fnins.2023.1179011
44. Jessen KR, Arthur-Farraj P (2019) Repair Schwann cell update: adaptive reprogramming, EMT, and stemness in regenerating nerves. Glia 67(3):421–437. https://doi.org/10.1002/glia.23532
45. Jessen KR, Mirsky R (2016) The repair Schwann cell and its function in regenerating nerves. J Physiol 594(13):3521–3531. https://doi.org/10.1113/jp270874
46. Dong Z, Huo J, Liang A, Chen J, Chen G, Liu D (2021) Gamma-secretase inhibitor (DAPT), a potential therapeutic target drug, caused neurotoxicity in planarian regeneration by inhibiting Notch signaling pathway. Sci Total Environ 781:146735. https://doi.org/10.1016/j.scitotenv.2021.146735
47. Mahakkanukrauh P, Surin P, Vaidhayakarn P (2005) Anatomical study of the pudendal nerve adjacent to the sacrospinous ligament. Clin Anat (New York, NY) 18(3):200–205. https://doi.org/10.1002/ca.20084
48. van der Walt S, Oettlé AC, Patel HR (2015) Surgical anatomy of the pudendal nerve and its branches in South Africans. Int J Impot Res 27(4):128–132. https://doi.org/10.1038/ijir.2015.10
49. Qu Z, Chen B, Yang M, Chen Y, Ming S, Hou W (2023) Comparative study of two different rat models of stress urinary incontinence. Int Urogynecol J 34(12):2867–2872. https://doi.org/10.1007/s00192-023-05593-3